Cerium Oxyhydroxide Clusters: Formation, Structure, and Reactivity

Frederic Aubriet and Jean-Jacques Gaumet

Laboratoire de Spectrométrie de Masse et Chimie Laser, Institut Jean Barriol Fédération de Recherche 2843, Université Paul Verlaine-Metz, Metz, France

Wibe A. de Jong

Pacific Northwest National Laboratory, Richland, Washington 99352

Gary S. Groenewold,* Anita K. Gianotto, and Michael E. McIlwain

Idaho National Laboratory, Idaho Falls, Idaho 83415

Michael J. Van Stipdonk and Christopher M. Leavitt

Wichita State University, Wichita, Kansas 67260

Received: February 19, 2009; Revised Manuscript Received: April 19, 2009

Cerium oxyhydroxide cluster anions were produced by irradiating ceric oxide particles by using 355 nm laser pulses that were synchronized with pulses of nitrogen gas admitted to the irradiation chamber. The gas pulse stabilized the nascent clusters that are largely anhydrous $[Ce_xO_y]$ ions and neutrals. These initially formed species react with water, principally forming oxohydroxy species that are described by the general formula $[Ce_xO_y(OH)_z]^-$ for which all the Ce atoms are in the IV oxidation state. In general, the extent of hydroxylation varies from a value of three OH per Ce atom when $x = 1$ to a value slightly greater than 1 for $x \geq 8$. The Ce_3 and Ce_6 species deviate significantly from this trend: the $x = 3$ cluster accommodates more hydroxyl moieties compared to neighboring congeners at $x = 2$ and 4. Conversely, the $x = 6$ cluster is significantly less hydroxylated than its $x = 5$ and 7 neighbors. Density functional theory (DFT) modeling of the cluster structures shows that the hydrated clusters are hydrolyzed, and contain one-to-multiple hydroxide moieties, but not datively bound water. DFT also predicts an energetic preference for formation of highly symmetric structures as the size of the clusters increases. The calculated structures indicate that the ability of the Ce_3 oxyhydroxide to accommodate more extensive hydroxylation is due to a more open, hexagonal structure in which the Ce atoms can participate in multiple hydrolysis reactions. Conversely the Ce_6 oxyhydroxide has an octahedral structure that is not conducive to hydrolysis. In addition to the fully oxidized (Ce(IV)) oxyhydroxides, reduced oxyhydroxides (containing a Ce(III) center) are also formed. These become more prominent as the size of the clusters increases, suggesting that the larger ceria clusters have an increased ability to accommodate a reduced Ce(III) moiety. In addition, the spectra offer evidence for the formation of superoxide derivatives that may arise from reaction of the reduced oxyhydroxides with dioxygen. The overall intensity of the clusters tends to monotonically decrease as the cluster size increases; however, this trend is interrupted at Ce_{13}, which is significantly more stable compared to neighboring congeners, suggesting formation of a dehydrated Keggin-type structure.

Introduction

The chemistry of cerium oxides is a topic of interest because material surfaces display pronounced activity for catalyzing a variety of processes, notably the water−gas shift reaction,[1,2] steam reforming of organics,[3,4] and oxidation reactions.[5−10] Fundamental processes include adsorption of neutral reactant molecules (such as CO, H_2O, CO_2, and H_2), and the breaking and formation of bonds, producing formate leading to eventual generation of methanol, formic acid, methyl formate, and other molecules. Optimization of these reactions is a desired goal to achieve improved yields, but requires a detailed knowledge of the reaction mechanism including details of kinetics and thermodynamics. Generating information at this level of detail on surfaces is a challenging task, which has motivated strong efforts to model cluster behavior using computational methods, and significant strides have been achieved using theory.[11−24] However, it is computationally difficult to model surface processes because of the large number of atoms that must be accommodated. For this reason clusters of atoms are modeled as surrogates for reactive sites on surfaces. However, modeling metal oxide clusters is not simple either, because for a given elemental composition, multiple structures are possible that have competitive formation enthalpies, which leads to ambiguity in correlating reaction chemistry with discrete molecules. In addition to catalytic interest, the cerium oxide clusters also form from hydrolysis and condensation reactions occurring in Ce(IV) solutions;[25] the details of the cluster formation processes are not known. These considerations provide motivation for performing experimental studies of clusters.

* To whom correspondence should be addressed. E-mail: gary.groenewold@inl.gov.

10.1021/jp9015432 CCC: $40.75
Published on Web 05/11/2009

An attractive approach for examining clusters is to form them in the gas phase, where there is the potential for control of the solvent environment. The difficulty in doing so, particularly with metal oxides, is that clusters do not readily volatilize. Two general approaches may be used, electrospray ionization and sputter desorption. While electrospray has been used to examine lanthanide coordination complexes,[26−39] there are fewer examples for generation of cluster ions with multiple metal cations. Salient examples of the use of electrospray include the work on alumina clusters by Sarpola and co-workers,[40−42] and more recently on uranium oxides by Pemberton.[43−45] Clusters formed in this manner tend to be ionically bound and have an inner solvation sphere that is complete or nearly so. Sputter desorption can employ either projectiles (neutral or charged atoms or molecules) or laser pulses. In the projectile category, Gianotto and Groenewold investigated a variety of aluminum, silicon, and chromium oxides, generating small-to-medium sized cluster ions with rhenium tetroxide (ReO_4^-) as the projectile.[46−53] Laser ablation is more commonly used, and Aubriet[54−58] and Gaumet[59−63] have used it for forming alumina, silica, and d-block oxyanions. Laser irradiation has also enjoyed extensive use for forming metal oxide clusters by targeting the laser on a rotating metal rod as pioneered by several groups,[64−71] enabling study of a wide variety of transition metal oxides; this approach tends to form hypo-oxidized species, and the extent of oxidation can be manipulated by seeding the ablation region with oxygen. Formation of cluster ions with heavier metals (e.g., f elements) has not been widely explored, but pioneering work by Gibson has used laser ablation to generate oxide cluster cations of both lanthanide and transition metals,[72−74] and in one instance noted a propensity for attachment of H_2O to cations,[74] which is germane to the present study. Gibson and Haire also showed that a wide range of plutonium oxides were formed by using laser ablation,[75,76] but beyond these studies there have been few other experiments conducted to investigate oxide clusters of the f elements.

Our initial attempts to produce cerium oxide cluster ions via desorption using projectiles (ReO_4^- molecules)[77] in a quadrupole ion trap did not produce abundant secondary ions, and motivated the present study of the generation of cerium oxide ions with laser ablation. While only low abundance clusters were produced by the laser under high vacuum, application of a pulse of N_2 gas coincident with the laser pulse produced abundant anion clusters. This enabled investigation of the chemistry of the cerium oxide clusters in terms of composition and dissociation behavior, which was compared with computationally generated structures, as described herein.

Experimental Section

Generation of Cerium Complexes by Laser Ablation. Targets were generated by pressing powdered CeO_2 into a target press (Cerac Inc., Milwaukee, WI) and then mounting it in the sample holder. Samples were evacuated to between 20 and 30 mTorr prior to admission to the high vacuum chamber of the FT-ICR-MS.

Fourier Transform Ion Cyclotron Resonance Mass Spectrometry (FT-ICR-MS). Mass spectra were acquired in negative detection mode by using a laser desorption/ablation ionization (LDI)/(LA)-FT-ICR mass spectrometer (IonSpec, Lake Forest, CA) equipped with an actively shielded 9.4-T superconducting magnet (Cryomagnetics, Oak Ridge, TN). The external ion source ProMaldi card was used. Particles were pressed onto a sample holder prior to introduction into the source region of the mass spectrometer. Ions were generated by laser ablation (LA) of the sample with an ORION air-cooled Nd:YAG laser system (New Wave Research Inc., Fremont, CA) working at the 355 nm wavelength (laser pulse duration 5 ns, output energy 4 mJ). The ions resulting from 8 successive laser-sample interactions were stored in a RF-only hexapole before being transferred to the FT-ICR cell, which was maintained at a background pressure of 6×10^{-10} Torr. There were 200 ms between pulses. After each pulse, the sample stage was moved such that ions were generated from a fresh (not previously ablated) target area. Stage motion is on the order of 100−200 μm. An ion guide situated between the LA stage and the FT-ICR cell was tuned to allow ions in the 200−1200 m/z range to be efficiently transferred into the FT-ICR-MS cell. To observe the highest mass clusters, the ion transfer parameters were modified to increase the transfer/trapping efficiency of the high m/z range ions. To thermalize ions during accumulation in the storage hexapole N_2 was introduced by a pulsed valve, which was opened for 1.8 s, allowing ion stabilization prior to transfer to the FT-ICR-MS cell. After transfer, ions were trapped in the ICR cell with a 0.2 V trapping potential. The pressure in the FT-ICR-MS was on the order of 5×10^{-10} Torr, as measured with an ion gauge located near the throat of a turbomolecular pump. The pressure inside the FT-ICR-MS cell during trapping and all subsequent manipulations is not known, but is probably close to that measured with the ion gauge because of the open design and high conductance of the cell. Nevertheless, because the cell is located further from the turbo pump than the ion gauge, pressures in the cell could be modestly higher. Trapped ions are excited by the application of an arbitrary excitation wave function on the excitation plates. The resulting image current was detected, amplified, digitized, apodized (Blackman), and Fourier-transformed to produce a mass spectrum. The signal was sampled during 2.097 s with 4096 K data points. The obtained mass accuracy was typically better than 1 ppm, and the mass resolution ($m/\Delta m$) at m/z 500 was close to 100 000. Mass measurements were made at very high resolution (e.g., 1 000 000 at m/z 931.5) to confirm compositional assignments when required.

Tandem mass spectrometry measurements were performed by isolating the ion of interest, using a stored waveform inverse Fourier transform (SWIFT) sequence,[78] which ejected all species except those having the desired mass. Ion kinetic energy was then increased by using sustained off-resonance irradiation collision-induced dissociation (SORI-CID),[79] resulting in collisions with nitrogen that was introduced into the FT-ICR-MS via a pulsed valve opened for 10 ms during the SORI event. The SORI frequency offset (1.5% of the parent ion cyclotron frequency) was applied for 250 ms.

Additional LA-MS experiments were performed with a Bruker Reflex IV MALDI-TOF instrument (Bruker-Franzen Analytik GmbH, Bremen, Germany) equipped with a delayed extraction. Ionization was achieved with use of a nitrogen laser (λ = 337 nm, pulse duration 3 ns, output energy 400 μJ, repetition rate 5 Hz). The laser spot size diameter is ~30 μm. The laser fluence was varied by means of an attenuator from 22 to 540 mJ/cm^2, producing irradiance values varying between 7.3×10^6 and 1.8×10^8 W/cm^2. The mass spectrometer was operated in the reflectron mode at a total acceleration voltage of 20 kV and a reflecting voltage of 23 kV. Mass spectra are the sum of 100 laser shots, each targeting a fresh area of the sample surface. This was done to avoid variation of the mass spectrum resulting from laser matter interaction that could produce a significant alteration of the composition as well as the physical and chemical properties. The ion assignment is

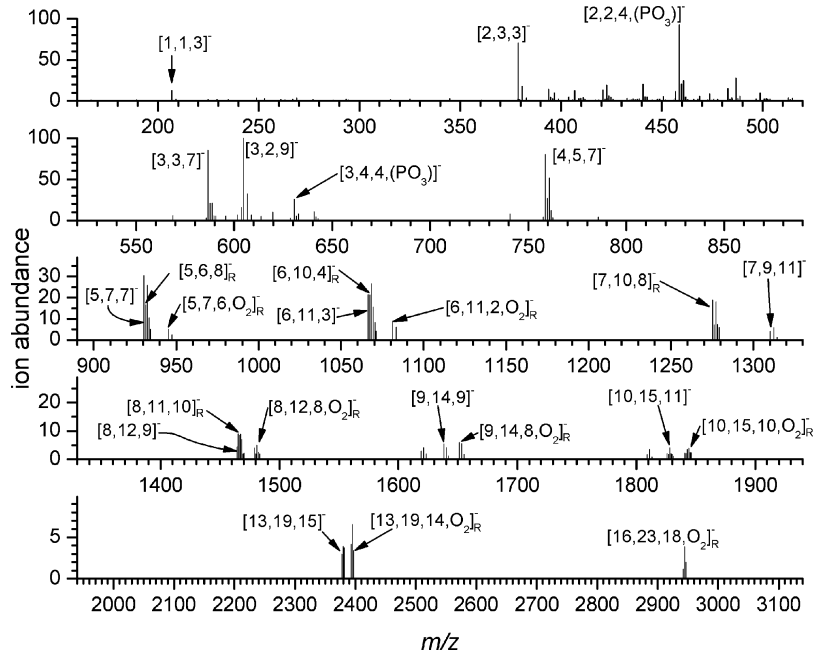

Figure 1. Negative ion laser ablation mass spectrum of cerium oxide, recorded by using the FT-ICR-MS, applying a N_2 pulse coincident with the laser. Only selected ions are labeled, and a complete listing is found in Table S1 in the Supporting Information. Compositions denoted with an "R" are reduced, and contain a Ce(III) center.

attained after external calibration performed with polyethylene glycol (PEG) 600 and/or PEG 1500, using the Na^+ and K^+ cationized ions.[80]

Molecular Structure and Frequency Calculations with Density Functional Theory. DFT calculations with the NWChem suite of programs[81,82] were performed by using the Stuttgart small core relativistic effective core potential (RSC ECP, 28 electrons in the core) and associated Stuttgart orbital basis set for cerium,[83−90] and the valence triple-ζ plus polarization (TZVP) DFT optimized basis sets for oxygen and hydrogen.[91] In all cases, spherical basis sets were employed. Geometry optimization and frequencies (plus zero-point energy corrections) were calculated by using the LDA functional,[92,93] while B3LYP[94,95] was used to calculate binding energies.

Results and Discussion

The application of a pulse of N_2 gas coincident with the laser impact produced numerous abundant higher mass clusters that contained up to 16 cerium atoms (Figure 1, also Table S1 in the Supporting Information). The most prominent ion series in the smaller ion envelopes are compositionally described as oxyhydroxides having the structural formula $[Ce_xO_y(OH)_z]^-$, where $x = (2y + z - 1)$, and for which all Ce atoms are in the IV oxidation state. Within this paper, these formulas are referred to by using $[x,y,z]^-$ designations, where x, y, and z refer to the numbers of Ce atoms, oxo, and hydroxo moieties, respectively. This formula as written carries with it structural connotation, specifically that hydroxyl groups are present on the clusters, as opposed to datively bound H_2O, or hydride moieties. This is consistent with the idea that water present in the hexapole ion accumulation chamber reacts with the dehydrated Ce_xO_y cluster anions by hydrolysis, forming hydroxyl groups, similar to what was observed with alumina,[48,49,53] silica,[52] and chromia[46] oxyanions in the gas phase, and is supported by DFT calculations (vide infra) which showed that hydroxyl-containing structures were indeed lowest in energy.

A second ion series consists of the reduced oxyhydroxides, which are distinct from the oxidized versions in that one of the Ce atoms in these clusters can be considered to be reduced to the III oxidation state. A third significant ion series is the superoxides, whose formulas can be generated by substitution of O_2 for OH in many of the elemental compositions of the fully oxidized oxyhydroxides. By assuming the presence of a superoxide moiety, the oxidation state of Ce in this ion series is +4.0, the same as in the fully oxidized oxyhydroxides; alternatively, restricting oxygen to the −2 state would require hyperoxidized cerium, which is unlikely; we note that Schwarz and co-workers produced $[CeO_2]^+$, which is formally a Ce(V) species;[96] however, it underwent reduction in gas phase ion−molecule reactions. The superoxide complexes are likely formed from the reaction of reduced oxyhydroxide or oxide species with dioxygen via a redox condensation, and by reaction of neutral clusters with O_2^-. The former process is supported by condensation of $[CeO_2]^-$ with O_2 (vide infra) and by prior studies of vanadyl and reduced uranyl coordination complexes that have been shown to undergo redox condensations with dioxygen in the gas phase.[97,98] In addition to these three families of ions, several other types of ions are formed that are related to the fully oxidized oxyhydroxide ion series by "substitution" of hydroxide by other anions, such as ethoxide, acetate, or PO_3^-. The alternative anions are derived from surface contaminants that are present on the sample, and were also indicated by the positive ion mass spectrum that contained C, H, and O atoms consistent with organic acid surface contamination.

The formation of cluster ions containing a large number of hydroxyl groups was unexpected, since prior laser ablation experiments of metal oxides showed that one or at most two OH groups were present in anion and cation clusters.[99−101] In the present LA experiments, large cluster anions are formed by ejection of Ce_xO_y species into the gas phase[73,80] that are stabilized by collisions with the pulse gas. The Ce_xO_y species may be ionic or neutral, and may exist in their ground state or in an excited state. Ionization of the neutral clusters occurs by (i) reaction with electrons or small anions (OH^-, O^-, O_2^-, OEt^-, OAc^-, PO_3^-) in the LA-induced plume or (ii) the fragmentation of excited neutrals by means of the heterolytic bond rupture.[80] The

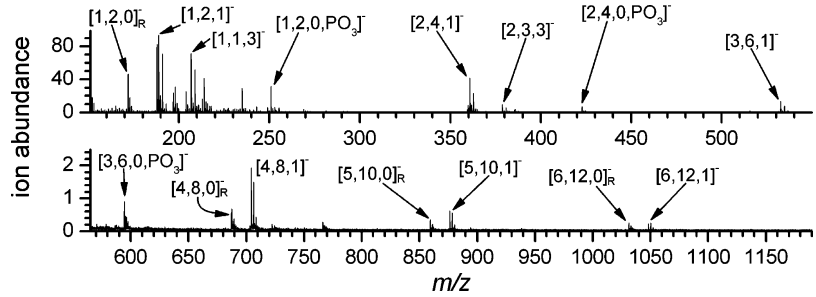

Figure 2. Negative ion laser ablation mass spectrum of cerium oxide, recorded by using the ToF-MS. In this experiment, pressures in the target region, and ion lifetimes, are much lower than those in the target region of the FT-ICR-MS shown in Figure 1. Compositions denoted with an "R" are reduced, and contain a Ce(III) center.

initially formed cluster ions are dehydrated, but react with water to form highly hydroxylated molecules in the ion accumulation hexapole where the ions spend several seconds before being injected into the FT-ICR-MS cell. The hydrolysis of cerium oxyanions with adventitious water present in the background atmosphere is analogous to hydrolysis of Al, Si, and Cr oxyanions seen in quadrupole ion traps.[46,48,52] This mechanism would require a higher pressure of water vapor and substantial ion lifetimes, conditions that are met in the accumulation hexapole of the FT-ICR-MS. Upon addition of the gas pulse, transient pressures of 10^{-4} to 10^{-5} Torr are reached, and the time between the beginning of ion accumulation in the hexapole and transfer to the FTICR cell is about 2 s. The stabilizing effect of the gas pulse is underscored by observation of abundant, highly hydroxylated oxyhydroxides, which readily dehydrate with modest excitation (vide infra).

The oxyhydroxide ion formation mechanism was supported by a lower pressure LA experiment, in which the time between the formation and the detection of ions is shorter and the in-source pressure is lower. These conditions should produce ions that are less extensively hydroxylated. Ion emission under these conditions was examined by analysis of CeO_2 with use of a LA-ToF-MS, making the assumption that the species initially produced by laser-material interactions will be unaffected by the mass analyzer.[102] The ToF mass spectrum contains ion series that correspond to the fully oxidized oxyhydroxides $[Ce_xO_y(OH)_z]^-$, only in this case z never exceeded 3 and usually had a value of 1 (Figure 2). Thus the number of hydroxyl moieties in these clusters is much fewer than in the clusters generated in the FT-ICR-MS experiments, where ions are produced that are much more extensively hydroxylated. Significant reduced $[Ce_xO_{2x}]^-$ anions (designated with a subscripted R in the figures) are also observed in the ToF spectra that were lower in intensity or not observed in LA-FTICRMS experiments. The intensities of the reduced $[Ce_xO_{2x}]^-$ anions increase as x goes from 3 to 6, compared to the intensities of the corresponding oxidized $[Ce_xO_{2x}(OH)_1]^-$ anions, to the point where the reduced species is the most intense ion in the Ce_6 envelope. These observations underscore the importance of reduced $[Ce_xO_{2x}]^-$ ions in the LA plume.

The fact that the O_2-containing species are also observed in the ToF-MS analyses suggests that these are formed by reactions of O_2^- with neutral clusters. However, we note that these are not as prominent as in the higher pressure FT-ICR-MS experiment, which indicates that some of the cluster anions, i.e., the reduced species, are being converted to O_2-containing species by reaction with O_2. This conclusion was further supported by direct observation of dioxygen condensation with the reduced $[CeO_2]^-$ cluster (vide infra).

Another important difference between the two experiments is that the intensities of the larger clusters formed under low-pressure conditions of the ToF are generally lower, which suggests that not only are the hydrated species stabilized by the gas pulse, but so also are the initially formed Ce_xO_y clusters (neutral and ionized). The LA-ToF mass spectrum shows that the intensities of the Ce_x ion envelopes decrease with size, a pattern that is not always overtly apparent in the FT-ICR-MS experiments, because the latter are perturbed by temporal gating of the ion guide leading to the ICR cell, which is adjustable depending on the mass of the ions to be trapped. Nevertheless, the FT-ICR-MS data do show that the overall intensities of the high-mass clusters generally decrease with increasing size, except for the Ce_1 clusters, which are lower abundance due to the timing of the ion guide gating, and the Ce_{13} clusters, which are more intense than their neighboring congeners. This suggests augmented stability for the Ce_{13} clusters. The molecules containing surface contaminants become significantly less important with increasing cluster size.

To gain perspective on ion formation tendencies, the propensity for formation of the fully oxidized oxyhydroxide, reduced oxyhydroxide, and superoxide ion families was examined as a function of cluster size, using the N_2 gas-pulse experiments in the FT-ICR-MS. A qualitative evaluation of the relative importance of the fully oxidized and reduced oxyhydroxide and superoxide families is shown by a plot of their fractional abundances within the individual Ce_x envelopes (Figure 3). By using the Ce_4 reduced oxyhydroxides as an example, the intensities of all Ce_4 reduced oxyhydroxides are summed, and ratioed to the total abundance of the Ce_4 fully oxidized oxyhydroxides, reduced oxyhydroxides, and superoxides. This analysis shows that for $x \leq 4$, the fully oxidized oxyhydroxides (Figure 3, square data points) are predominant, but for greater x values, their fraction decreases to values between 0.2 and 0.4 for $x \geq 7$. The fraction of the fully oxidized oxyhydroxide values is variable in the $x = 10$, 11 envelopes, which reflects imprecision resulting from low overall ion abundances (and the $x = 12$ clusters were not observed at all). As the fully oxidized oxyhydroxides decrease, both the reduced oxyhydroxides and superoxides increase, which is consistent with the idea that a fraction of the reduced oxyhydroxides are converted to superoxides by redox condensation with dioxygen.[97,98]

However the reduced oxyhydroxides and superoxides do not maintain a constant ratio in the different ion envelopes. In the Ce_7 envelope, formation of the superoxides is strongly disfavored, while formation of the reduced oxyhydroxides is predominant. This suggests that the Ce_7-reduced oxyhydroxides are less reactive with the dioxygen. An alternative explanation is that the Ce_7 superoxides may further react with H_2O to form fully oxidized and reduced oxyhydroxides, which could deplete their abundances. The situation is exactly reversed in the Ce_{13} envelope, where effectively no reduced oxyhydroxides were

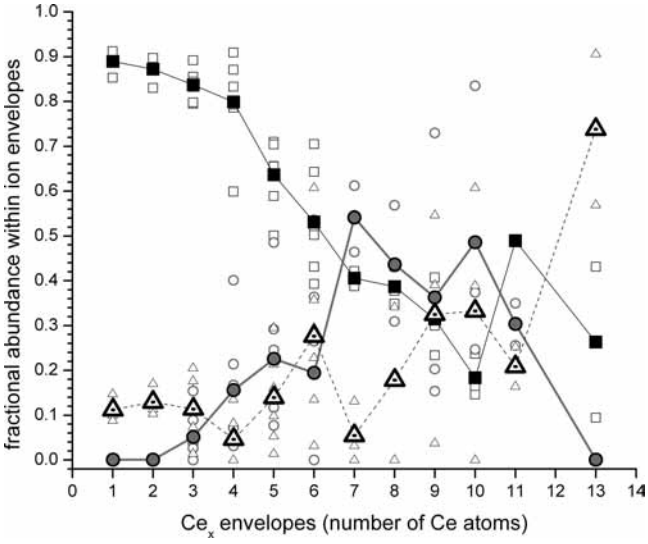

Figure 3. Fractional abundances of ion families within Ce_x ion envelopes. The fully oxidized oxyhydroxides are represented by squares, reduced oxyhydroxides by circles, and superoxides by triangles. Bold points connected by lines are averages, while small open points are individual data points.

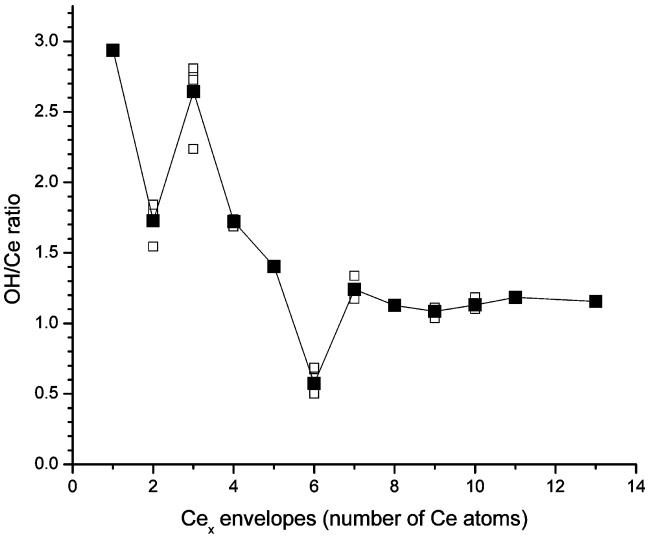

Figure 4. Hydroxide-to-cerium (OH/Ce) ratio in the fully oxidized oxyhydroxides plotted versus Ce_x ion envelope. Values are abundance-weighted in cases where multiple oxidized oxyhydroxides are present within individual ion envelopes. Larger, filled points are averages, open points are individual measurements.

formed, but instead the superoxides account for most of the ion intensity. These observations probably reflect variations in (a) the abilities of the reduced clusters to stabilize dioxygen versus a Ce(III) center that become pronounced for $x \geq 6$ and (b) the reactivity of the superoxides with water, leading to depletion of these species in the Ce_7 and Ce_{11} envelopes.

Species in the ion envelopes also display differences in their tendency to undergo hydrolysis, which is reflected in the hydroxide-to-cerium ratio (OH/Ce) in the fully oxidized oxyhydroxides (Figure 4). The Ce_1 envelope shows a value of nearly three, reflecting the preferential formation of $[CeO(OH)_3]^-$. For Ce_x envelopes having higher x values, OH/Ce values generally show a slow decrease toward ~1.1, with two salient discontinuities. The Ce_3 molecules display a remarkable tendency to accommodate H_2O, much more so compared to neighboring congeners. Conversely, Ce_6 clusters do not hydrolyze to the same extent as either Ce_5 or Ce_7 species, and the OH/Ce ratio

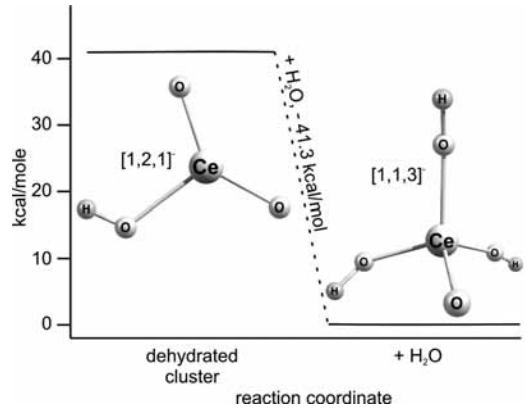

Figure 5. Reaction coordinate diagram and calculated ion structures for hydration of $[CeO_2(OH)]^-$ forming $[CeO(OH)_3]^-$.

for the Ce_6 envelope is low as a result. As the ion envelopes increase in size, the OH/Ce ratio is found to be near 1.1 to 1.2; note that the value for the highly stable Ce_{13} envelope is 1.15. These preferences will be discussed in the context of ion dissociation and computational modeling.

Ce_1 Complexes. Several low mass ions were recorded that corresponded to Ce_1 species, most notably the ion at *m/z* 206.9, which is $[1,1,3]^-$ in accord with the accurate mass measurement (Table S1 in the Supporting Information, Figure 1) and the fact that the predominant dissociation pathway is dehydration. DFT calculations generated a tetrahedral structure consistent with expression of the formula as $[CeO(OH)_3]^-$ (Figure 5) that required on the order of 40 kcal/mol for dehydration to form $[1,2,1]^-$. In fact a low abundance $[1,2,1]^-$ ion at *m/z* 188.9 was also recorded by using the FT-ICR-MS, and it was much more prominent in the LA-ToF experiment. Calculations for the $[1,2,1]^-$ molecule indicate a trigonal structure that is probably very susceptible to hydrolysis, consistent with the preference for the formation of $[1,1,3]^-$. A higher hydrate that would have a composition of $[CeO_5H_5]^-$ was not observed, indicating that Ce prefers to form four-coordinate anion structures in the gas phase. Calculations indicate tetrahedral geometry, a reasonable supposition in accord with similar to geometries previously calculated for Ce(halide)$_4$ molecules.[21]

Collision-induced dissociation reactions were also conducted on the superoxide derivative $[1,1,2,O_2]^-$, which showed elimination of H_2O (forming $[CeO_4]^-$) at low excitation energies, but at higher energies both H_2O and O_2 were eliminated, forming the reduced $[1,2,0]^-$ molecule at *m/z* 171.9. Isolation of $[1,2,0]^-$ for 10 s resulted in conversion of ~15% of the ions to $[1,2,0,O_2]^-$, which occurred via reaction with trace O_2 present in the FT-ICR-MS. Dissociation of $[1,2,0,O_2]^-$ occurred by loss of O_2. DFT modeling of the $[1,2,0,O_2]^-$ molecule showed that the lowest energy structure contained two oxo ligands, and a side-on bound O_2 moiety (Figure 6). This structure would be consistent with the coordination expected for a peroxide ligand. However, if that were the case, then the formal oxidation state of the Ce atom would be +5. A more reasonable explanation is that the O_2 moiety is a side-on bound superoxide ligand, analogous to those identified as products of reduced uranyl ($[U(V)O_2]^+$) and dioxygen.[103,104] The second lowest energy structure contained two oxo ligands, and a superoxide bound in a more conventional end-on arrangement. Three other structural alternatives were significantly higher in energy.

Ce_2 Complexes. The most abundant Ce_2 species at *m/z* 378.8 had an accurate mass consistent with the structural composition $[2,3,3]^-$. Collision-induced dissociation of $[2,3,3]^-$ occurred by

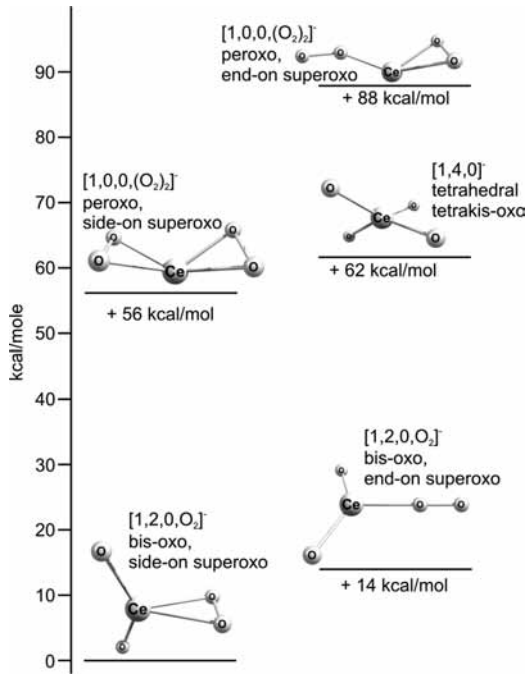

Figure 6. Structures and relative energies calculated for the $[CeO_4]^-$ molecules.

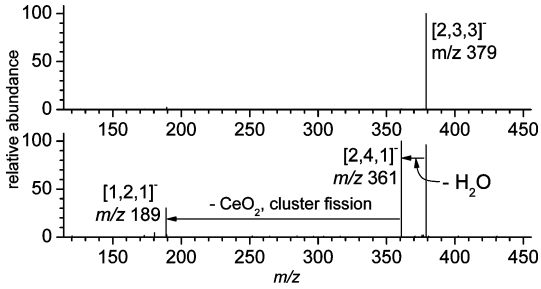

Figure 7. Collision-induced dissociation of $[Ce_2O_3(OH)_3]^-$, $[2,3,3]^-$: top, isolation of *m/z* 379; bottom, dissociation at $V_{SORI} = 2$ V (excitation).

SCHEME 1: Dissociation Reactions of $[2,3,3]^-$

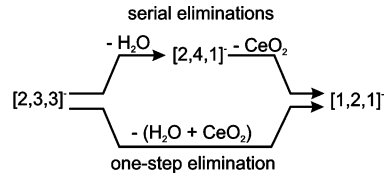

dehydration forming $[2,4,1]^-$, which is seen at low abundance in the MS-1 spectrum, and also formed $[1,2,1]^-$ by loss of (H_2O + CeO_2) (Figure 7, Scheme 1). The latter loss is termed cluster fission, and could occur directly (perhaps losing a $CeO(OH)_2$ neutral) or by the serial losses of H_2O and CeO_2. Both dehydration and cluster fission occurred with modest excitation of $[2,3,3]^-$, requiring only $V_{SORI} \approx 2$ V (Figure S1, Supporting Information). In contrast, if the intermediate $[2,4,1]^-$ dehydration product was cooled by inserting a second isolation-activation event, then the cluster fission reaction required much more energy, not being observed until V_{SORI} exceeded 12 V in the second event. This indicates that the $[2,4,1]^-$ is very resistant to cluster fission, which suggests formation of $[1,2,1]^-$ directly from $[2,3,3]^-$. During the extra time needed for the second isolation/excitation event (an additional 2 s), the $[2,4,1]^-$ may undergo radiative cooling or isomerization to a structure more stable with respect to cluster fission. Another alternative is that $[2,3,3]^-$ may rearrange and eliminate CeO_2, forming $[1,1,3]^-$ sufficiently activated that it spontaneously eliminates H_2O to provide the observed $[1,2,1]^-$. Since $[1,1,3]^-$ is not seen in the CID spectrum of $[2,3,3]^-$, we think this is less likely, but the explanation cannot be excluded on the basis of these experiments.

Theory is in accord with a single structure for $[2,3,3]^-$: calculations indicate a rhombic structure (Figure 8), similar to those predicted for analogous aluminum, silicon, titanium, and chromium species.[46,52,53,105] The calculations predict that dehydration to form $[2,4,1]^-$ would require ~40 kcal/mol, and that the product would retain the rhombic structure, as attempts to generate alternative structures (which require a Ce═O moiety) were not successful. Cluster fission of $[2,4,1]^-$ to produce $[1,2,1]^-$ and CeO_2 was calculated to require an additional 64.8 kcal/mol.

A low abundance ion at *m/z* 396.8 was also formed, having an accurate mass consistent with $[2,2,5]^-$, indicating that $[2,3,3]^-$ reacts further with one additional water. DFT predicted that this too would have a stable rhombic structure, and that the second hydration step would be exothermic by about 20 kcal/mol. Maintaining the rhombic core would entail formation of a *gem*-triol moiety on one side of the molecule, consistent with its somewhat lower stability. The fact that this is not a more abundant ion in the mass spectrum indicates that kinetics are limiting the extent of hydration in the cluster ions that are observed. This suggests that in some cases the cerium oxyhydroxide clusters may well be able to thermodynamically accommodate additional hydrolysis, but the products of these reactions are not observed because condensation kinetics tend to slow down as hydration of metal centers proceeds.[48,50]

Lower abundance ions observed at *m/z* 393.8, 406.8, and 420.8 can be rationalized in terms of substitution of hydroxide in the $[2,3,3]^-$ molecule by superoxide, ethoxide, and acetate, respectively, and have accurate masses consistent with those assignments. The superoxide is denoted $[2,3,2,O_2]^-$, and collisionally dissociates by dehydration forming $[2,4,0,O_2]^-$, in a process that was calculated to require 32.3 kcal/mol. Dehydration of the superoxide was accompanied by cluster fission producing $[1,2,0,O_2]^-$ at *m/z* 203.9; the latter ion was also produced by dehydration of the $[1,1,2,O_2]^-$ molecule (vide supra). The $[1,2,0,O_2]^-$ eliminates O_2, as noted above. As in the case of the Ce_1 superoxides, the O_2 moiety prefers side-on coordination (Figure 9), only in this case, O_2 is more stable when bridging the two metal centers. The calculations predict that the Ce−O bond distances for the dangling oxygen atoms are very nearly the same (1.86−1.87 Å) suggesting that electrons are delocalized among the O atoms in these molecules. In aggregate, the O atoms in the Ce_2 superoxides must be oxidized, otherwise Ce would be forced into an oxidation state >+4. The abundant Ce_2-bearing ion at *m/z* 458.8 contains phosphate, as indicated by the accurate mass measurement, and by the observation of $[PO_3]^-$ in the low mass region of the mass spectrum. The phosphate is evidently a contaminant of the CeO_2 target, since we do not see it in the analysis of other samples, and it was also detected in the LA-ToF experiments. As in the lower mass Ce_2 ions, a ring-bearing structure is indicated by the composition, and the intensity of the ion suggests that the Ce_2-phosphate cluster $[2,2,4,(PO_3)]^-$ molecule is very stable, which is consistent with the fact that it was resistant to cluster fission, instead undergoing only losses of one and two H_2O molecules when excited to dissociation.

Ce_3 Complexes. Ce_3-containing complexes are formed at *m/z* values ranging from ~530 to ~630, and display a more rich array of possible ions compared to those of the Ce_2 and Ce_1

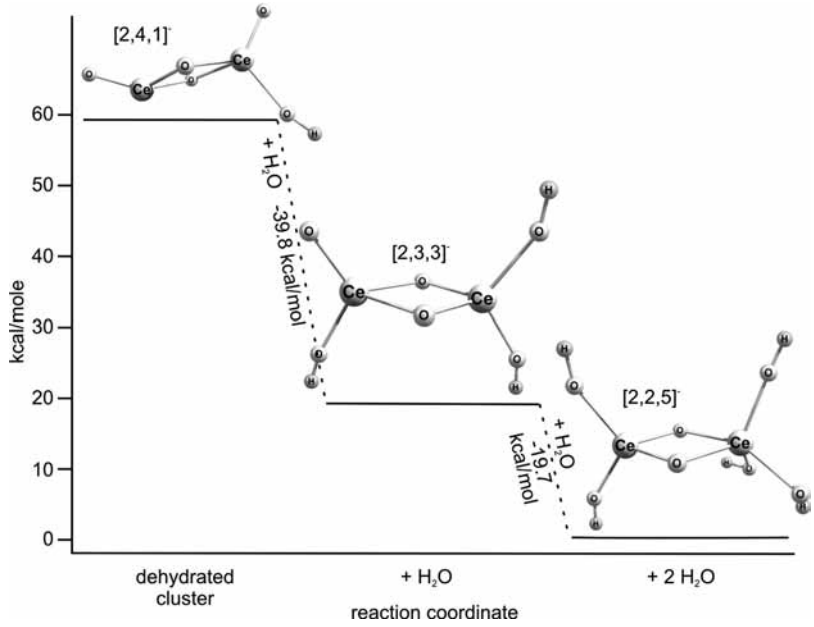

Figure 8. Reaction coordinate diagram and structures of reactants and products calculated for Ce_2 species undergoing hydration. Processes shown are $[2,4,1]^- + H_2O \rightarrow [2,3,3]^-$ and $[2,3,3]^- + H_2O \rightarrow [2,2,5]^-$.

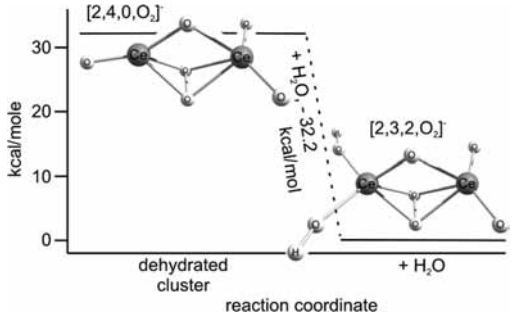

Figure 9. Reaction coordinate diagram and structures of reactant and product calculated for Ce_2 oxyhydroxide species undergoing hydration. The process shown is $[2,4,0,O_2]^- + H_2O \rightarrow [2,3,2,O_2]^-$.

ion envelopes. The $[3,2,9]^-$ fully oxidized oxyhydroxide constitutes one of the more abundant ions in the mass spectrum, and is related to the $[3,3,7]^-$, $[3,4,5]^-$, $[3,5,3]^-$, and $[3,6,1]^-$ by hydration/dehydration reactions. The salient feature of the Ce_3 ion envelope is the pronounced ability to accommodate water, to a much greater extent than any of the Ce_2 ions, or any ions having a larger number of Ce atoms. Kinetic arguments derived from differing ion lifetimes in the ion accumulation hexapole are not satisfactory to explain this very different behavior, principally because both the Ce_2 and Ce_4 ion envelopes are formed under exactly the same conditions, and neither of these have comparable propensities for addition of H_2O. Computational modeling of the $[3,3,7]^-$ suggests stabilization resulting from the formation of intramolecular hydrogen bonds; however, as of this writing models for the $[3,2,9]^-$ had not yet been completed, and so the unusual ability of the Ce_3 clusters for accommodation of H_2O has not been satisfactorily rationalized.

Dehydration of the hydrated, fully oxidized oxyhydroxides was demonstrated by collision-induced dissociation studies of $[3,3,7]^-$, which resulted in facile elimination of one, two, and three H_2O molecules at low V_{SORI} values (Figure S2 in the Supporting Information and Scheme 2). In series with the dehydration reactions were two cluster fission reactions that eliminated one and two CeO_2 molecules forming $[2,4,1]^-$ and $[1,2,1]^-$, but hydrated versions of these ions were not formed. All five of these product ions could be observed at very low

SCHEME 2: Dissociation Reactions of $[3,3,7]^-$

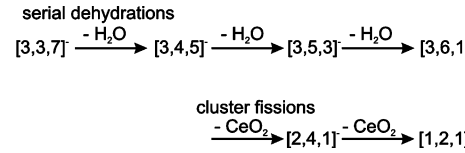

excitation voltages. The $[3,6,1]^-$ product resulting from elimination of all three H_2O molecules may be significantly condensed, and when this ion was isolated after dehydration, we were unable to induce cluster fission, even at $V_{SORI} = 16$ V. The observation of a dehydrated cluster stable to cluster fission is analogous to that seen in the dissociation of the $[2,3,3]^-$ fully oxidized oxyhydroxide, and in fact is common to all of the cerium oxyhydroxide systems. The intriguing question posed is why is cluster fission achievable starting from the extensively hydroxylated $[3,3,7]^-$ parent ion, but not after isolating the triply dehydrated $[3,6,1]^-$ product. In this case, formation of the $[2,4,1]^-$ cannot be achieved by a reasonable loss of a single molecule from $[3,3,7]^-$, and thus serial dehydration/cluster fission reactions must be responsible. The fact that $[3,6,1]^-$ cannot be activated to cluster fission once it is isolated suggests that the ion is either vibrationally cooled during the second isolation/activation step, making energies necessary to cause cluster fission unattainable, or it undergoes an isomerization to form a highly condensed structure that is resistant to cluster fission. Alternatively, cluster fission may be competitive with dehydration in $[3,3,7]^-$: elimination of CeO_2 or $CeO(OH)_2$ would produce $[2,1,7]^-$ and $[2,2,5]^-$, respectively, and these ions may not be stable with respect to dehydration when formed in this manner.

The DFT calculations of the $[3,3,7]^-$ isomer predicted two stable structures, a hexagonal structure bridged by a μ_3-OH moiety, and a bis-rhombus containing *gem*-triol moieties on both terminal Ce atoms, which was 20.1 kcal/mol higher in energy (Figure 10). Calculated interatomic distances suggest that the μ_3-hydroxo moiety in the $[3,3,7]^-$ hexagonal structure may be stabilized by intramolecular hydrogen bonding. Elimination of H_2O from $[3,3,7]^-$ produces $[3,4,5]^-$, for which four different structures were calculated to be stable. The lowest was a

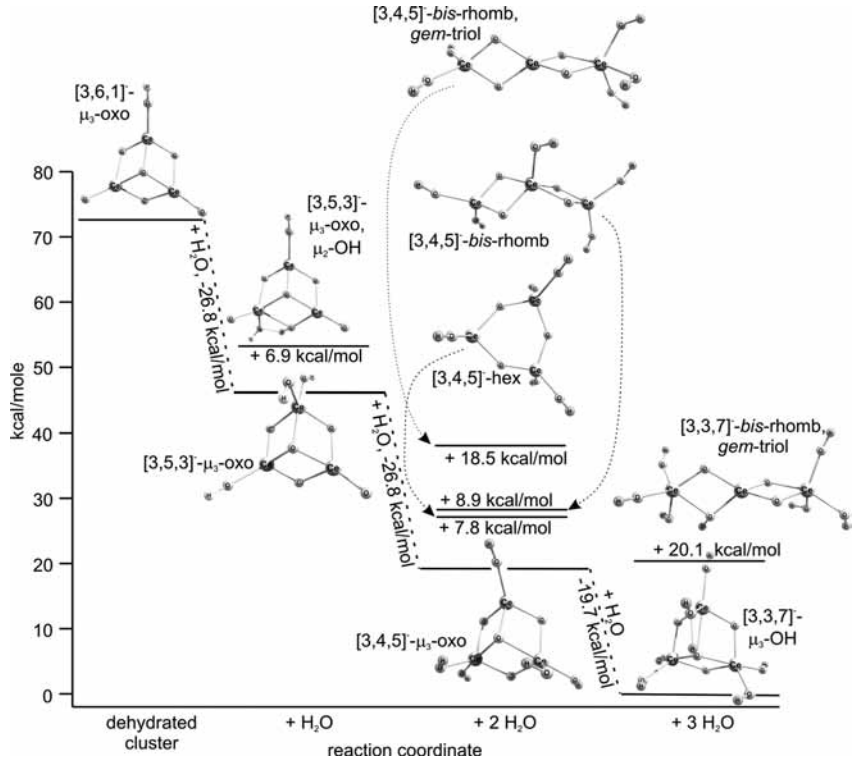

Figure 10. Reaction coordinate diagram and structures for the Ce_3 oxyhydroxides.

hexagonal structure with a μ_3-oxo bridge; however, a nonbridged hexagon and a bent double rhombus were only 7.8 and 8.9 kcal/mol higher, respectively. Loss of a second H_2O generated $[3,5,3]^-$, but in this case only μ_3-oxo-hexagons were calculated, the double rhombus structures being no longer competitive. Similarly, loss of the third H_2O produces $[3,6,1]^-$, and in this case a single structure was identified, a μ_3-oxo-hexagon. The energies required for elimination of the three H_2O molecules from the oxo-bridged hexagonal structures are on the order of 20−30 kcal/mol, and the values do not increase dramatically as the ion approaches dehydration. A total of 73.3 kcal/mol is required for elimination of the three H_2O molecules, and an additional 80.9 kcal/mol to induce cluster fission of the $[3,6,1]^-$. Interestingly, cluster fissions of $[3,5,3]^-$ and $[3,4,5]^-$ are slightly less energetically expensive, but products of these eliminations are not observed. Thus, cluster fission is not occurring in the Ce_3 ion envelope while the much more favorable dehydration reactions are still available.

As in the case of the Ce_1 and Ce_2 ion envelopes, Ce_3 species were observed in which a hydroxide has been substituted by a superoxide, ethoxide, or PO_3^-. Dissociation of the $[3,4,4,O_2]^-$ superoxide at *m/z* 583.7 resulted in two serial dehydration reactions to form $[3,5,2,O_2]^-$ and $[3,6,0,O_2]^-$, and this was accompanied by subsequent loss of O_2 to form $[3,6,0]^-$ at *m/z* 515.7 via a reductive elimination in which one Ce atom in the product ion can be viewed as reduced to the +3 oxidation state (Figure S3, Supporting Information). This suggests that the Ce_3 oxy cluster is better able to accommodate an electron compared to $Ce_{1,2}$ ions. No cluster fission was observed in the $[3,4,4,O_2]^-$ dissociation experiments. A particularly abundant phosphate-containing ion at *m/z* 630.7 is formed and can be written with the structural formula $[3,4,4,(PO_3)]^-$. Dissociation studies were consistent with this formula, in that the ion eliminated two H_2O molecules to form $[Ce_3O_6(PO_3)]^-$ at *m/z* 594.7, and underwent a concurrent cluster fission losing an additional CeO_2 to form a stable product ion at *m/z* $[Ce_2O_4(PO_3)]^-$ (Figure S4, Supporting Information), which is the dehydrated version of the $[Ce_2O_3(PO_3)(OH)_2]^-$ ion at *m/z* 440.8.

Ce_4 Complexes. The most abundant Ce_4 species was $[4,5,7]^-$ at *m/z* 758.6, although both hydrated and dehydrated versions of this ion are also formed at *m/z* 776.6 and 740.6, respectively, which correspond to $[4,4,9]^-$ and $[4,6,5]^-$. The abundance of $[4,5,7]^-$ is significantly greater than either $[4,4,9]^-$ or $[4,6,5]^-$, suggesting that either the kinetics of formation are more favorable, or that the structure is fairly stable. Interestingly the intensities of the ethoxide and phosphate derivatives in the Ce_4 ion envelope are substantially lower compared with those of Ce_{1-3}, which suggests that formation of the larger clusters involves atoms lying below the ceria surface, where surface contaminants are not directly attached. The Ce_4 ion envelope also contains substantial abundances of reduced ions having the composition $[4,4,8]^-$, signaling the ability of these clusters to accommodate a Ce(III) metal center.

The structural formula of the $[4,5,7]^-$ ion was supported by ion dissociation experiments. Like the Ce_2 and Ce_3 oxyhydroxides, the molecule fragmented at very low excitation voltages by eliminating all possible (three) H_2O molecules forming $[Ce_4O_8(OH)]^-$ at *m/z* 704.6, which was accompanied by cluster fission eliminations of one, two, and three CeO_2 molecules (Figure S5, Supporting Information). Fragmentation of $[4,5,7]^-$ was accomplished by using very low ion excitation energy (V_{SORI} = 0.5 V), and showed that while ~40% of the product ions were accounted for by the dehydration reactions, >20% were the result of cluster fission, the latter accounting for a larger fraction than had been seen for the Ce_2 or Ce_3 clusters. This implies that this cluster may be less stable compared to neighboring congeners in the Ce_{2-3} ion envelopes. At greater excitation energies, the fraction of the ions as intact parents decreased, but the relative abundances of the dehydration and cluster fission products did not appreciably change. When the dissociation cascade was interrupted by isolating the triply dehydrated product $[4,8,1]^-$ at *m/z* 704.6, further attempts to

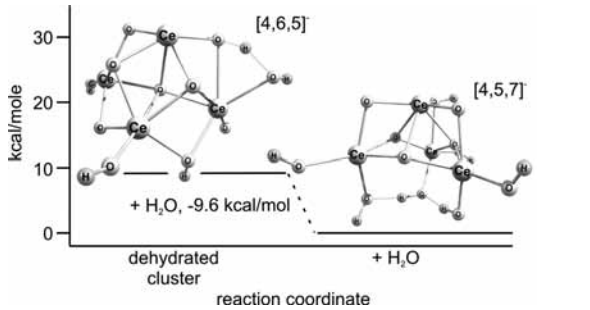

Figure 11. Structures and reaction coordinate diagram for two Ce_4 species, related by a modestly exothermic hydration reaction.

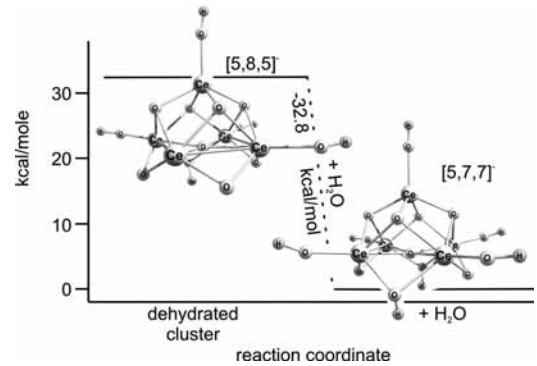

Figure 12. Structures and reaction coordinate diagram for $[5,5,7]^-$ and the dehydration congener $[5,8,5]^-$.

induce dissociation were unsuccessful, at excitation energies as high as $V_{SORI} = 12$ V. As in the case of the smaller, fully oxidized oxyhydroxides, dehydration followed by ion isolation results in stabilization with respect to cluster fission.

The dissociation studies of the Ce_4 species occurred just after a sample change, which meant that the base pressure in the FT-ICR-MS was slightly increased, probably as a result of a trace amount of H_2O vapor emanating from the oxide surface. This afforded the opportunity to see whether the $[4,8,1]^-$ would add H_2O back, which is an important phenomenon related to hypothesized ion formation processes. After formation by collision-induced elimination of three H_2O, $[4,8,1]^-$ was isolated and then allowed to react with ambient H_2O vapor present in the FT-ICR-MS. The ion could be observed to smoothly add first one and then two H_2O molecules, forming $[4,7,3]^-$ and then $[4,6,5]^-$ at *m/z* 722.6 and 744.6, respectively (Figure S6, Supporting Information). The kinetics for the H_2O additions followed those expected for serial bimolecular reactions, and modeled as such by using the approach developed for hydration of alumina cluster anions.[48] The base pressure in the FT-ICR-MS (6×10^{-10} Torr as measured by the ion gauge, see the Experimental Section) was assumed to consist entirely of H_2O, which would be equivalent to a number density of 1.9×10^7 molecules/cm^3. The modeled rate constants were $k_1 = 1 \times 10^{-9}$ and $k_2 = 3 \times 10^{-10}$ cm^3 s^{-1} molecule^{-1}, which would be about 50% and 10% efficient compared to values calculated by using reparameterized average dipole orientation theory.[106−112] This shows that the partial pressure of H_2O cannot be lower than a factor of 2 less than that recorded by the ion gauge, but more importantly that $[4,8,1]^-$ and $[4,7,3]^-$ show significant hygroscopic behavior. We believe that this behavior is probably general for many of the other cerium oxyhydroxides, and perhaps for other cerium oxygenated cluster anions (phosphates, alkoxides, and superoxides).

The structures calculated for $[4,5,7]^-$ and $[4,6,5]^-$ were both polyhedra decorated with multiple pendant oxo or hydroxo moieties (Figure 11). The $[4,6,5]^-$ structure contains a particularly interesting μ_4-oxo bridge connected to all four Ce atoms, which evidently is hydrolyzed upon reaction with H_2O since it is not observed in the $[4,5,7]^-$ structure. The fact that addition of H_2O to $[4,6,5]^-$ only results in a 9.6 kcal/mol advantage in formation of $[4,5,7]^-$ suggests that the structure is approaching a point where further hydrolysis does not occur. In fact Ce atoms in both structures are more highly coordinated than are the monomeric species (where tetrahedral coordination is preferred). The $[4,5,7]^-$ structure can be viewed as a Ce_3O_3 hexagon that is capped by a CeO_2OH^-, which the capping Ce atom is directly coordinated to each of the ring O atoms, and bound to each of the ring Ce atoms by a μ_2-oxo or μ_2-hydroxo bridge. On the opposite side of the Ce_3O_3 hexagon, the $[4,5,7]^-$ structure is stabilized by intramolecular hydrogen bonding between the pendant hydroxo moieties.

A small superoxide ion at *m/z* 755.6 having the composition $[4,5,6,O_2]^-$ was isolated and dissociated (Figure S7, Supporting Information), which revealed serial losses of one and two H_2O, followed by loss of dioxygen, finally forming the reduced species $[4,8,0]^-$ at *m/z* 687.6, a dissociation pattern analogous to that seen for the Ce_3 superoxide cluster.

Ce_5 Complexes. The Ce_5 ion envelope contains only one abundant, fully oxidized oxyhydroxide, the $[5,7,7]^-$ at *m/z* 930.5; neither abundant dehydrated nor abundant hydrated versions of this ion are formed. As in the case of the Ce_4 ion envelope, a significant reduced ion is observed, which has the composition $[5,6,8]^-$. The dissociation pattern observed from the fully oxidized $[5,7,7]^-$ was in accord with the structural formula, in that at low excitation energies three H_2O molecules were eliminated, together with cluster fission eliminations of one, two, three, and four CeO_2 molecules (Figure S8, Supporting Information). Use of higher excitation energies did not appreciably change the fraction of ions partitioned into the cluster fission and dehydration channels, although the fraction of intact parent ions decreased. We had insufficient intensity to isolate the fully dehydrated ions, and hence knowledge is lacking regarding whether or not these became more resistant to dissociation upon cooling in the FT-ICR-MS cell. In addition to dehydration, a minor fragmentation pathway was observed that corresponded to loss of three H_2O plus one OH, producing a reduced anion having the composition $[5,10,0]^-$ at *m/z* 859.5; in this process the leaving hydroxide is oxidized to the radical, which requires that the remaining ion is reduced by one electron. This elimination suggests that the Ce_5 oxyhydroxide has an enhanced ability to accommodate a Ce(III) metal center compared to the smaller oxyanions, where elimination of an OH radical does not occur.

The structures calculated for the Ce_5 species begin to assume a higher level of symmetry (Figure 12). The $[5,7,7]^-$ molecule has what is very close to D_{2h} symmetry, with four Ce atoms forming a square planar base, in which the metals are coordinated by a μ_4-oxo, and alternating μ_2-oxo and μ_2-hydroxo bridges. This base is capped by the fifth Ce atom, which is coordinated to the four metal atoms in the square Ce_4 base by four μ_3-oxo moieties. The structure of the monodehydrated $[5,8,5]^-$ was also calculated, and found to be very similar to that of the $[5,7,7]^-$, lacking a pendant OH on one of the Ce metal centers. The non-OH coordinated Ce atom may be fairly reactive, since the $[5,8,5]^-$ is not seen in the mass spectrum generated directly from laser ablation, but only in the MS/MS experiment. The DFT calculations showed hydration of the $[5,8,5]^-$ to be exothermic by 32.8 kcal/mol.

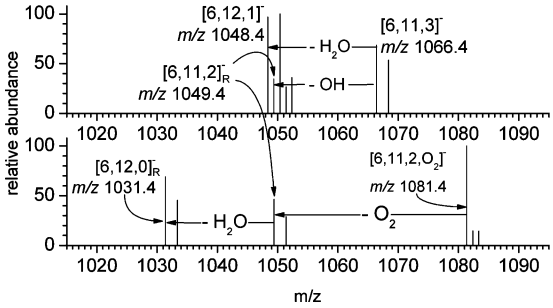

Figure 13. Collision-induced dissociation of Ce_6-containing cluster anions: top, dissociation of *m/z* 1066.4, $[6,11,3]^-$ at $V_{SORI} = 10$ V (cluster fission products not shown); bottom, dissociation of $[6,11,2,O_2]^-$ at $V_{SORI} = 2$ V.

A relatively abundant $[5,7,6,O_2]^-$ is seen at *m/z* 945.5, corresponding to the superoxide derivative of $[5,7,7]^-$. The fact that the superoxide was formed suggests a precursor capable of accommodating a Ce(III) metal center, and undergoing one-electron oxidation with dioxygen in forming the superoxide complex. This is consistent with the fact that the fully oxidized oxyhydroxide eliminated a OH radical forming a reduced oxyhydroxide, which are also seen in the mass spectrum. The $[5,7,6,O_2]^-$ eliminated one, two, and three H_2O forming $[Ce_5O_{10}(O_2)]^-$ (Figure S9, Supporting Information), and also lost ($3H_2O + O_2$) to form the reduced $[Ce_5O_{10}]^-$ ion in a low abundance process analogous to the loss of ($3H_2O + OH$) from $[Ce_5O_7(OH)_7]^-$.

Ce_6 Complexes. The fully oxidized $[6,11,3]^-$ oxyhydroxide at *m/z* 1066.4 is the most abundant ion formed in the Ce_6 envelope; however, there are also substantial ions corresponding to the reduced oxyhydroxide $[6,10,4]^-$ at *m/z* 1067.4 and a superoxide $[6,11,2,O_2]^-$ at 1081.4. These compositions indicate that ions in the Ce_6 envelope are substantially less hydroxylated compared to clusters having either smaller or larger numbers of Ce atoms. Since the Ce_6 oxyhydroxides are formed under exactly the same conditions as the other clusters, which are substantially more hydroxylated, we conclude that this cluster has a much lower tendency for hydrolysis. Dissociation of $[6,11,3]^-$ resulted in elimination of a single H_2O, forming $[6,12,1]^-$ at *m/z* 1048.4 (Figure 13, top), and was accompanied by a cluster fission resulting in losses of one to five CeO_2 units, ultimately forming $[1,2,1]^-$. In addition, the fully oxidized $[6,11,3]^-$ loses a hydroxyl radical, which necessitates reduction of the Ce_6 core in producing the reduced $[6,11,2]^-$ at *m/z* 1047.4. The average Ce oxidation number in the $[6,11,2]^-$ is 3.8, as compared to 4.0 for the other cluster ions in the Ce_6 ion envelope. This suggests that like the Ce_5 clusters, the Ce_6 oxyhydroxides effectively accommodate a Ce(III) metal center.

DFT modeling suggests a structure for $[6,11,3]^-$ in which the Ce atoms comprise a slightly distorted octahedron (Figure 14). A second stable structure was identified 18.4 kcal/mol higher in which five of the Ce atoms comprise a square pyramid that is modified by addition of CeO_2 to one of the trigonal faces (referred to as "side-on"). Hydration of the octahedron was predicted to be exothermic by 38.1 kcal/mol, and produces a $[6,10,5]^-$ structure for which all Ce atoms except one have a pendant hydroxide; however, despite the favorable calculated energetics, this ion was only present in very low abundance, suggesting that its formation was kinetically limited. A $[6,10,5]^-$ side-on structure analogous to that for $[6,11,3]^-$ side-on structure was also calculated to be stable, although ~13 kcal/mol higher than the isomeric octahedron. A second hydration step was also predicted to be exoergic by 13.4 kcal/mol, but the product $[6,9,7]^-$ was not seen in the mass spectrum. The calculated structure suggests that this hydration step would require formation of a *gem*-diol moiety on one of the Ce metal centers on the octahedron, which is evidently slow enough that it is not observed.

A surprisingly abundant superoxide-containing cluster was observed at *m/z* 1081.4, corresponding to the structural formula $[6,11,2,O_2]^-$. This ion suggests formation of a reactive reduced $[6,11,2]^-$ (seen from loss of OH radical from $[6,11,3]^-$ above) in the laser ablation plume that is condensed with dioxygen, forming the superoxide complex. An alternative explanation may be the formation of a superoxide anion $[6,12,0,O_2]^-$ by reaction between O_2 and the reduced $[6,12,0]^-$ (produced by laser ablation) followed by hydration reaction to yield $[6,11,2,O_2]^-$. This structural formula was supported by collision-induced dissociation, which showed initial loss of neutral dioxygen producing $[6,11,2]^-$ at *m/z* 1049.4, followed in series by loss of H_2O to form $[6,12,0]^-$ (Figure 13, bottom). The fact that loss of O_2 preceded loss of H_2O was surprising because H_2O had been the most easily eliminated neutral in previous superoxide systems. The favored redox elimination of O_2 in this system further supports the idea that the Ce_6 cluster ions have the ability to stabilize a Ce(III) metal center to a much greater degree than do the smaller clusters.

Ce_7 Complexes. The Ce_7 ion envelope contained a low abundance *m/z* 1274.3 that corresponds to the fully oxidized $[7,11,7]^-$, which is accompanied by a more intense ion at *m/z* 1275.3 that is reduced $[7,10,8]^-$. The structure calculated for $[7,11,7]^-$ showed Ce atoms positioned symmetrically in D_{5h} symmetry (Figure 15). μ_3-Oxo bridges connect each of the five equatorial Ce atoms to four adjacent Ce atoms, and the two axial Ce atoms to all five equatorial Ce atoms. In addition, the two axial Ce atoms were bound to each other by a μ_2-oxo bridge through the center of the structure; this oxygen atom is not calculated to interact with any of the equatorial metals. The reduced $[7,10,8]^-$ ion at *m/z* 1275.3 is slightly more abundant than the fully oxidized $[7,11,7]^-$. The abundance of the reduced $[7,10,8]^-$ again suggests the ability of the larger clusters to stabilize a Ce(III) metal center. The peak at *m/z* 1312.3 corresponded to fully oxidized $[7,9,11]^-$ that is related to the $[7,11,7]^-$ by the addition of two H_2O molecules. Curiously there is no intermediate oxidized $[7,10,9]^-$, which indicates that the Ce_7 may be partitioned into two populations that have dissimilar abilities to accommodate hydrolysis.

Ce_x Complexes, $x = 8-13$. Cerium clusters for Ce_{8-11} had compositions corresponding to fully oxidized and reduced oxyhydroxides and to the corresponding superoxides. The fully oxidized oxyhydroxides had OH/Ce ratios that hovered between 1.1 and 1.2, displaying none of the variability seen in the Ce_3 or Ce_6 ion envelopes (Figure 4). The relative abundances of the reduced oxyhydroxides within the individual ion envelopes become greater than that of the corresponding fully oxidized ions, and the oxyhydroxides also become relatively less abundant, as shown in Figure 3. The absolute ion abundances decrease steadily as the number of Ce atoms increases above Ce_8, to the point where Ce_{12} clusters are not significantly above background. The monotonic decrease in intensities is interrupted, however, by the abundant ion envelope for Ce_{13}, which indicates that the Ce_{13} ions are more stable neighboring congeners. Given the trend toward reduced species seen in the Ce_{8-11} ion envelopes, it was surprising that the Ce_{13} ion envelope did not contain any reduced oxyhydroxides, instead only the fully oxidized $[13,19,15]^-$ was formed. However, the most abundant Ce_{13} ion was the superoxide $[13,19,14,O_2]^-$, which may be

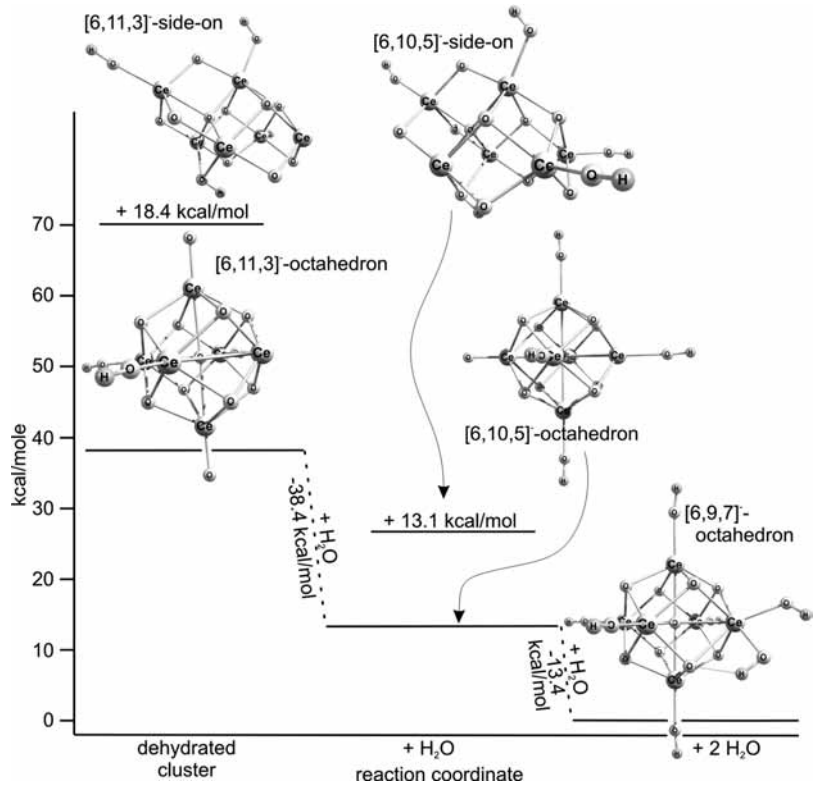

Figure 14. Structures and reaction coordinate diagram for $[6,11,3]^-$ undergoing addition of one and two H_2O to form $[6,10,5]^-$ and $[6,9,7]^-$.

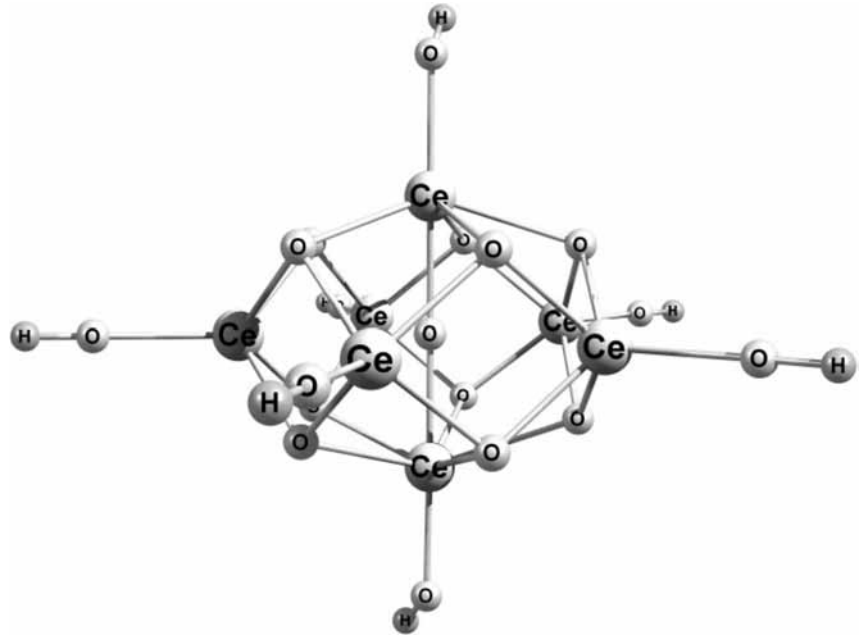

Figure 15. Structure of $[7,11,7]^-$ calculated with DFT.

formed from a redox condensation of the reduced $[13,19,14]^-$ with dioxygen or by serial O_2 and H_2O additions of a dehydrated reduced precursor as suggested for the Ce_6 clusters. Finally, a low abundance, but above background ion was measured at *m*/*z* 2944.4, which would correspond to $[16,23,18,O_2]^-$. The fact the neighboring congeners were not formed indicates that this composition also enjoys unusual stability.

Dissociation experiments were not performed for the $Ce_{x>7}$ ion clusters because ion abundances were low; however, elucidating the fragmentation behavior and structures of these clusters remains a worthy target for future research. The surprising intensity of the Ce_{13} clusters $[13,19,15]^-$ and $[13,19,14,(O_2)]^-$ does suggest formation of structures of higher stability, perhaps Ce analogues of a Keggin structure well-known for Group 6 transition metals (notably W) and also Al. A charge neutral Ce Keggin would have the structural formula $[(CeO_4)(Ce_{12}O_8(OH)_{28}]°$, and when ionized by attachment of a hydroxide would form $[13,12,29]^-$, using the notation of this paper. Exactly seven dehydration reactions of $[13,12,29]^-$ would produce the observed $[13,19,15]^-$; however, if this were occurring then the absence of any of the higher hydrates is puzzling. An alternative concept might be direct LA formation of a $[13,19,15]^-$ Ce Keggin that can accommodate additional water molecules, but is not further hydrated because of slow

addition kinetics and weak binding, perhaps suggesting datively bound water, in which case the hydrated version should be rather written as $[13,15,19,(H_2O)_7]^-$. DFT calculations, which are challenging given the range of possible structures and the expense of calculations of systems of this size, are currently underway. Strategies to investigate this hypothesis are needed for better understanding of these intermediate-sized clusters.

Conclusions

Cerium oxyhydroxides are an intriguing class of molecules on account of their possible catalytic potential, and due to the fact that they provide insight into the difficult problem of oxypolymer formation in solutions of f elements in the +4 oxidation state. The study of discrete species has historically been difficult; however, in the present case a number of cerium oxyhydroxide clusters have been formed in the gas phase environment of a trapped ion mass spectrometer by using laser ablation with a coincident pulse of N_2 gas, which stabilizes nascent cluster ions. A low-pressure laser ablation experiment conducted with a time-of-flight mass spectrometer showed that only very low abundance, mostly dehydrated cluster ions were formed, a stark contrast to the gas-pulse LA experiment in the FT-ICR-MS. This suggests the following: (a) LA results in emission of both neutral and ionized Ce_xO_y cluster ions having a range of sizes, together with small neutral molecules and small ions; (b) the neutral clusters are ionized by reaction with the charged moieties, either electrons or small anions notably OH^- or O_2^-; (c) the cluster anions are stabilized by collisions with the N_2 gas; and (d) the cluster anions react with adventitious H_2O by hydrolysis to form oxyhydroxide species, or by reaction with O_2 to form superoxides. The reverse of these processes was demonstrated by collisionally activated dissociation that produced loss(es) of one or more H_2O molecules, accompanied by cluster fission reactions occurring in tandem with the dehydration reactions. Interruption of the dissociation cascade after the dehydration reactions allows the intermediate ions to deactivate, and subsequent reactivation of the cooled ions does not result in resumption of the cluster fission reactions, suggesting that the ions produced by dehydration are highly stable. The high stability was further suggested by extensive DFT calculations that showed that H_2O elimination required anywhere from 10 to ~40 kcal/mol, and that cluster fission required on the order of 80 kcal/mol.

Distributions of ions within the different $Ce_{x=1-13}$ ion envelopes varied considerably with x, and showed that as x increased, the number of hydroxyl moieties per Ce atom decreased, approaching 1 at values ≥7, suggesting that a OH "surface" density on the clusters is similar to what would be seen on a ceria surface is being approached. Ions having x values of 3 and 6 do not follow this general trend. The Ce_3 ion envelope is significantly more hydroxylated than would be expected, pointing to a structure capable of accommodating more hydrolysis than expected (implying a less-condensed structure that is likely hexagonal). Conversely, the Ce_6 ion envelope eschews hydrolysis as indicated by oxyhydroxide compositions that have a significantly fewer number of hydroxyl moieties, probably as a result of preferential formation of an octahedral structure. Limitations associated with slow hydration kinetics for the Ce_6 species may temper this conclusion; however, the Ce_6 clusters were formed under conditions identical to the neighboring Ce_5 and Ce_7, which strongly suggests hydration chemistry that is much different.

Once x becomes greater than 4, the relative abundances of reduced oxyhydroxide clusters become much more significant, as do those of the superoxides. This is consistent with the hypothesis that initially formed, reduced oxyhydroxides undergo a redox condensation with dioxygen, forming the superoxide complexes, but also may be due to slower reaction rates for homolytic reactions with water resulting from the larger size of the molecules. In general, the abundances of the ion envelopes fall monotonically as x increases; however, this pattern is interrupted at $x = 13$, and perhaps $x = 16$: these clusters are significantly more stable than are neighboring congeners having other numbers of Ce atoms.

DFT calculations of the clusters show an energetic preference for highly symmetrical structures as defined by the Ce atoms. Structures calculated for the Ce_2 ion envelope are modifications of a Ce_2O_2 rhombus. The most stable Ce_3 structures contain a Ce_3O_3 hexagon, which tends to accommodate additional oxo moieties by additional μ-oxo bridges, and is unusually susceptible to hydrolysis. The Ce atoms in the structures for the clusters in the Ce_4 ion envelope define an approximate tetrahedron, and are bound by μ-oxo bridges. The Ce atoms in the lowest energy structure for the Ce_5 oxyhydroxide define a square pyramid that is notable because it contains a centrally situated μ_4-oxo bridge at the center of the base. Octahedral structures that account for the most stable species in the Ce_6 envelope, and similarly the Ce_7, appear to be best represented by a related D_{5h} structure. The unusual stability of the Ce_{13} oxyhydroxides may be accounted for by formation of a Ce Keggin-type complex; however, this represents an ongoing research question.

These structural variations clearly manifest in terms of large alterations in the chemistry, in terms of reactivity with H_2O, ability to undergo reduction, and subsequent redox condensation with dioxygen. The variations may provide insight into reactivity of active sites on surfaces that are important in effecting catalytic transitions, and we expect that the ability to form these species will provide an entrée to studies of a wider range of ion−molecule reactions designed to simulate heterogeneous adsorption, hydrolysis, oxidation, and reduction.

Acknowledgment. Work by G. S. Groenewold and A. K. Gianotto was supported by the U.S. Department of Energy, and the INL Laboratory Directed Research & Development Program under DOE Idaho Operations Office Contract DE-AC07-05ID14517. W. A. de Jong's research was performed in part using the Molecular Science Computing Facility in the William R. Wiley Environmental Molecular Sciences Laboratory, a national scientific user facility sponsored by the U.S. Department of Energy's Office of Biological and Environmental Research located at the Pacific Northwest National Laboratory, which is operated for the Department of Energy by Battelle. F. Aubriet and J. J. Gaumet acknowledge supported by the University of Metz and the Ministere de l'Education Nationale, de la Recherche et de la Technologie (France). M. J. Van Stipdonk and C. M. Leavitt were supported in part through a grant from the U.S. National Science Foundation (CAREER-0239800).

Supporting Information Available: Accurate mass measurement and composition information (Table S1), complete listings of atom coordinates calculated for the complexes (Tables S2−S25), a plot of MS/MS ion abundance versus excitation energy (Figure S1), and additional MS/MS spectra (Figures S2−S10). This material is available free of charge via the Internet at http://pubs.acs.org.

References and Notes

(1) Qi, X. M.; Flytzani-Stephanopoulos, M. *Ind. Eng. Chem. Res.* **2004**, *43*, 3055.

(2) Shan, W. J.; Shen, W. J.; Li, C. *Chem. Mater.* **2003**, *15*, 4761.
(3) Papavasiliou, J.; Avgouropoulos, G.; Ioannides, T. *Catal. Commun.* **2004**, *5*, 231.
(4) Sharma, S.; Hilaire, S.; Vohs, J. M.; Gorte, R. J.; Jen, H. W. *J. Catal.* **2000**, *190*, 199.
(5) Hocevar, S.; Batista, J.; Levec, J. *J. Catal.* **1999**, *184*, 39.
(6) Hocevar, S.; Krasovec, U. O.; Orel, B.; Arico, A. S.; Kim, H. *Appl. Catal.* **2000**, *28*, 113.
(7) Martinez-Arias, A.; Fernandez-Garcia, M.; Soria, J.; Conesa, J. C. *J. Catal.* **1999**, *182*, 367.
(8) Zhu, T. L.; Kundakovic, L.; Dreher, A.; Flytzani-Stephanopoulos, M. *Catal. Today* **1999**, *50*, 381.
(9) Shibasaki, M.; Yoshikawa, N. *Chem. Rev.* **2002**, *102*, 2187.
(10) Tobisch, S. *J. Am. Chem. Soc.* **2005**, *127*, 11979.
(11) Gellings, P. J.; Bouwmeester, H. J. M. *Catal. Today* **2000**, *58*, 1.
(12) Hunt, P. A. *Dalton Trans.* **2007**, 1743.
(13) Adamo, C.; Barone, V. *J. Comput. Chem.* **2000**, *21*, 1153.
(14) Adamo, C.; Maldivi, P. *Chem. Phys. Lett.* **1997**, *268*, 61.
(15) Berny, F.; Muzet, N.; Troxler, L.; Dedieu, A.; Wipff, G. *Inorg. Chem.* **1999**, *38*, 1244.
(16) Clavaguera, C.; Dognon, J. P.; Pyykko, P. *Chem. Phys. Lett.* **2006**, *429*, 8.
(17) Cundari, T. R.; Sommerer, S. O.; Strohecker, L. A.; Tippett, L. *J. Chem. Phys.* **1995**, *103*, 7058.
(18) Guillaumont, D. *J. Phys. Chem. A* **2004**, *108*, 6893.
(19) Joubert, L.; Picard, G.; Legendre, J. J. *Inorg. Chem.* **1998**, *37*, 1984.
(20) Kuchle, W.; Dolg, M.; Stoll, H. *J. Phys. Chem. A* **1997**, *101*, 7128.
(21) Lanza, G.; Fragala, I. L. *J. Phys. Chem. A* **1998**, *102*, 7990.
(22) Lesar, A.; Muri, G.; Hodoscek, M. *J. Phys. Chem. A* **1998**, *102*, 1170.
(23) Perrin, L.; Maron, L.; Eisenstein, O. *Faraday Discuss.* **2003**, *124*, 25.
(24) Schurhammer, R.; Erhart, V.; Troxler, L.; Wipff, G. *J. Chem. Soc., Perkin Trans. 2* **1999**, 2423.
(25) Nash, K. L.; Sullivan, J. C. Kinetics of Complexation and Redox Reactions of the Lanthanides in Aqueous Solutions. In *Handbook on the Physics and Chemistry of Rare Earths*; Gschneidner, K. A., Jr., Eyring, L., Eds.; Elsevier Science Pbulishers, B.V.: Amsterdam, The Netherlands, 1991; Vol. 15, p 347.
(26) Groenewold, G. S.; Gianotto, A. K.; Cossel, K. C.; Van Stipdonk, M. J.; Oomens, J.; Polfer, N.; Moore, D. T.; de Jong, W. A.; McIlwain, M. E. *Phys. Chem. Chem. Phys.* **2007**, *9*, 596.
(27) Beer, P. D.; Brindley, G. D.; Fox, O. D.; Grieve, A.; Ogden, M. I.; Szemes, F.; Drew, M. G. D. *J. Chem. Soc., Dalton Trans.* **2002**, 3101.
(28) Chapon, D.; Husson, C.; Delangle, P.; Lebrun, C.; Vottero, P. J. A. *J. Alloys Compd.* **2001**, *323*, 128.
(29) Colette, S.; Amekraz, B.; Madic, C.; Berthon, L.; Cote, G.; Moulin, C. *Inorg. Chem.* **2003**, *42*, 2215.
(30) Colette, S.; Amekraz, B.; Madic, C.; Berthon, L.; Cote, G.; Moulin, C. *Inorg. Chem.* **2002**, *41*, 7031.
(31) Colton, R.; Klaui, W. *Inorg. Chim. Acta* **1993**, *211*, 235.
(32) Crowe, M. C.; Kapoor, R. N.; Cervantes-Lee, F.; Parkanyi, L.; Schulte, L.; Pannell, K. H.; Brodbelt, J. S. *Inorg. Chem.* **2005**, *44*, 6415.
(33) Curtis, J. M.; Derrick, P. J.; Schnell, A.; Constantin, E.; Gallagher, R. T.; Chapman, J. R. *Inorg. Chim. Acta* **1992**, *201*, 197.
(34) Lau, R. L. C.; Jiang, J. Z.; Ng, D. K. P.; Chan, T. W. D. *J. Am. Soc. Mass Spectrom.* **1997**, *8*, 161.
(35) Lees, A. M. J.; Charnock, J. M.; Kresinski, R. W.; Platt, A. W. G. *Inorg. Chim. Acta* **2001**, *312*, 170.
(36) Marcalo, J.; Pires de Matos, A.; Evans, W. *Organometallics* **1997**, *16*, 3845.
(37) Platt, A. W. G.; Fawcett, J.; Hughes, R. S.; Russell, D. R. *Inorg. Chim. Acta* **1999**, *295*, 146.
(38) Stewart, I. I.; Horlick, G. *Anal. Chem.* **1994**, *66*, 3893.
(39) Zhang, J. J.; Zhang, W.; Luo, Q. H.; Mei, Y. H. *Polyhedron* **1999**, *18*, 3637.
(40) Hellman, H.; Laitinen, R. S.; Kaila, L.; Jalonen, J.; Hietapelto, V.; Jokela, J.; Sarpola, A.; Ramo, J. *J. Mass Spectrom* **2006**, *41*, 1421.
(41) Sarpola, A.; Hietapelto, V.; Jalonen, J.; Jokela, J.; Laitinen, R. S. *J. Mass Spectrom.* **2004**, *39*, 423.
(42) Sarpola, A.; Hietapelto, V.; Jalonen, J.; Jokela, J.; Laitinen, R. S.; Ramo, J. *J. Mass Spectrom.* **2004**, *39*, 1209.
(43) Somogyi, A.; Pasilis, S.; Pemberton, J. E. *Int. J. Mass Spectrom.* **2007**, *265*, 281.
(44) Pasilis, S.; Somogyi, A.; Herrmann, K.; Pemberton, J. E. *J. Am. Soc. Mass Spectrom.* **2006**, *17*, 230.
(45) Pasilis, S. P.; Pemberton, J. E. *Inorg. Chem.* **2003**, *42*, 6793.
(46) Gianotto, A. K.; Hodges, B. D. M.; Benson, M. T.; Harrington, P. d. B.; Appelhans, A. D.; Olson, J. E.; Groenewold, G. S. *J. Phys. Chem. A* **2003**, *107*, 5948.
(47) Gianotto, A. K.; Hodges, B. D. M.; Harrington, P. B.; Appelhans, A. D.; Olson, J. E.; Groenewold, G. S. *J. Am. Soc. Mass Spectrom.* **2003**, *14*, 1067.
(48) Gianotto, A. K.; Rawlinson, J. W.; Cossel, K. C.; Olson, J. E.; Appelhans, A. D.; Groenewold, G. S. *J. Am. Chem. Soc.* **2004**, *126*, 8275.
(49) Gowtham, S.; Lau, K. C.; Deshpande, M.; Pandey, R.; Gianotto, A. K.; Groenewold, G. S. *J. Phys. Chem. A* **2004**, *108*, 5081.
(50) Gresham, G. L.; Gianotto, A. K.; Harrington, P. d. B.; Cao, L.; Scott, J. R.; Olson, J. E.; Appelhans, A. D.; Van Stipdonk, M. J.; Groenewold, G. S. *J. Phys. Chem. A* **2003**, *107*, 8530.
(51) Groenewold, G. S.; Kessinger, G. F.; Scott, J. R.; Gianotto, A. K.; Appelhans, A. D.; Delmore, J. E.; Avci, R. *Anal. Chem.* **2001**, *73*, 226.
(52) Groenewold, G. S.; Scott, J. R.; Gianotto, A. K.; Hodges, B. D. M.; Kessinger, G. F.; Benson, M. T.; Wright, J. B. *J. Chem. Phys. A* **2001**, *105*, 9681.
(53) Scott, J. R.; Groenewold, G. S.; Gianotto, A. K.; Benson, M. T.; Wright, J. B. *J. Phys. Chem., A* **2000**, *104*, 7079.
(54) Aubriet, F.; Poleunis, C.; Bertrand, P. *Appl. Surf. Sci.* **2003**, *203*−*204*, 114.
(55) Aubriet, F.; Poleunis, C.; Chaoui, N.; Maunit, B.; Millon, E.; Muller, J.-F.; Bertrand, P. *Appl. Surf. Sci.* **2002**, *186*, 315.
(56) Aubriet, F.; Maunit, B.; Muller, J.-F. *Int. J. Mass Spectrom.* **2001**, *209*, 5.
(57) Aubriet, F.; Maunit, B.; Courrier, B.; Muller, J.-F. *Rapid Commun. Mass Spectrom.* **1997**, *11*, 1596.
(58) Chety-Gimondo, R.; Aubriet, F.; Millon, E.; Muller, J.-F. *Rapid Commun. Mass Spectrom.* **2004**, *18*, 2939.
(59) Lafargue, P. E.; Gaumet, J. J.; Muller, J. F. *Chem. Phys. Lett.* **1998**, *288*, 494.
(60) Gaumet, J. J.; Membrey, F.; Chambaudet, A. *C. R. Acad. Sci. Ser. II-B* **1996**, *322*, 507.
(61) Khitrov, G. A.; Strouse, G. F.; Gaumet, J.-J. *J. Am. Soc. Mass Spectrom.* **2004**, *15*, 260.
(62) Lafargue, P. E.; Gaumet, J. J.; Muller, J. F. *J. Mass Spectrom.* **1996**, *31*, 623.
(63) Lafargue, P. E.; Gaumet, J. J.; Muller, J. F.; Labrosse, A. *J. Mass Spectrom.* **1996**, *31*, 623.
(64) Jarrold, M. F. *J. Phys. Chem.* **1995**, *99*, 11.
(65) Leuchtner, R. E.; Harms, A. C.; Castleman, A. W. *J. Chem. Phys.* **1989**, *91*, 2753.
(66) Xing, X.; Tian, Z.; Liu, H.; Tang, Z. *J. Phys. Chem. A* **2003**, *107*, 8484.
(67) Bergeron, D. E.; Castleman, A. W.; Morisato, T.; Khanna, S. N. *Science* **2004**, *304*, 84.
(68) Kimble, M. L.; Castleman, A. W. *Int. J. Mass Spectrom.* **2004**, *233*, 99.
(69) Kimble, M. L.; Castleman, A. W., Jr.; Burgel, C.; Bonacic-Koutecky, V. *Int. J. Mass Spectrom.* **2006**, *254*, 163.
(70) Justes, D. R.; Mitric, R.; Moore, N. A.; Bonacic-Koutecky, V.; Castleman, A. W., Jr. *J. Am. Chem. Soc.* **2003**, *125*, 6289.
(71) Sambrano, J. R.; Gracia, L.; Andres, J.; Berski, S.; Beltran, A. *J. Phys. Chem. A* **2004**, *108*, 10850.
(72) Gibson, J. K. *J. Vac. Sci. Technol.* **1995**, 13.
(73) Gibson, J. K. *J. Phys. Chem.* **1994**, *98*, 11321.
(74) Gibson, J. K. *J. Appl. Phys.* **1995**, *78*, 1274.
(75) Gibson, J. K.; Haire, R. G. *J. Alloy. Compd.* **2001**, *322*, 143.
(76) Gibson, J. K.; Haire, R. G. *J. Alloy. Compd.* **2004**, *363*, 112.
(77) Groenewold, G. S.; Delmore, J. E.; Olson, J. E.; Appelhans, A. D.; Ingram, J. C.; Dahl, D. A. *Int. J. Mass Spectrom. Ion Processes* **1997**, *163*, 185.
(78) Marshall, A. G.; Wang, T.-C. L.; Ricca, T. L. *J. Am. Chem. Soc.* **1985**, *107*, 7893.
(79) Gauthier, J. W.; Trautman, T. R.; Jacobson, D. B. *Anal. Chim. Acta* **1991**, *246*, 211.
(80) Aubriet, F.; Muller, J. F. *J. Am. Soc. Mass Spectrom.* **2008**, *19*, 488.
(81) Aprà, E.; Windus, T. L.; Straatsma, T. P.; Bylaska, E. J.; de Jong, W.; Hirata, S.; Valiev, M.; Hackler, M.; Pollack, L.; Kowalski, K.; Harrison, R.; Dupuis, M.; Smith, D. M. A.; Nieplocha, J.; Tipparaju, V.; Krishnan, M.; Auer, A. A.; Brown, E.; Cisneros, G.; Fann, G.; Fruchtl, H.; Garza, J.; Hirao, K.; Kendall, R.; Nichols, J.; Tsemekhman, K.; Wolinski, K.; Anchell, J.; Bernholdt, D.; Borowski, P.; Clark, T.; Clerc, D.; Dachsel, H.; Deegan, M.; Dyall, K.; Elwood, D.; Glendening, E.; Gutowski, M.; Hess, A.; Jaffe, J.; Johnson, B.; Ju, J.; Kobayashi, R.; Kutteh, R.; Lin, Z.; Littlefield, R.; Long, X.; Meng, B.; Nakajima, T.; Niu, S.; Rosing, M.; Sandrone, G.; Stave, M.; Taylor, H.; Thomas, G.; van Lenthe, J.; Wong, A.; Zhang, Z. *NWChem*, A Computational Chemistry Package for Parallel Computers, Version 4.7 ed.; Pacific Northwest National Laboratory: Richland, WA, 2005.
(82) Kendall, R. A.; Apra, E.; Bernholdt, D. E.; Bylaska, E. J.; Dupuis, M.; Fann, G. I.; Harrison, R. J.; Ju, J.; Nichols, J. A.; Nieplocha, J.; Straatsma, T. P.; Windus, T. L.; Wong, A. T. *Comput. Phys. Commun.* **2000**, *128*, 260.

(83) Bergner, A.; Dolg, M.; Kuchle, W.; Stoll, H.; Preuss, H. *Mol. Phys.* **1993**, *80*, 1431.
(84) Dolg, M.; Stoll, H.; Preuss, H.; Pitzer, R. M. *J. Phys. Chem.* **1993**, *97*, 5852.
(85) Fuentealba, P.; Preuss, H.; Stoll, H.; Vonszentpaly, L. *Chem. Phys. Lett.* **1982**, *89*, 418.
(86) Fuentealba, P.; Vonszentpaly, L.; Preuss, H.; Stoll, H. *J. Phys. B: At., Mol. Opt. Phys.* **1985**, *18*, 1287.
(87) Igel-Mann, G.; Stoll, H.; Preuss, H. *Mol. Phys.* **1988**, *65*, 1321.
(88) Kaupp, M.; Schleyer, P. V.; Stoll, H.; Preuss, H. *J. Chem. Phys.* **1991**, *94*, 1360.
(89) Kuchle, W.; Dolg, M.; Stoll, H.; Preuss, H. *Mol. Phys.* **1991**, *74*, 1245.
(90) Kuchle, W.; Dolg, M.; Stoll, H.; Preuss, H. *J. Chem. Phys.* **1994**, *100*, 7535.
(91) Godbout, N.; Salahub, D. R.; Andzelm, J.; Wimmer, E. *Can. J. Chem.-Rev. Can. Chim.* **1992**, *70*, 560.
(92) Slater, J. C. *Phys. Rev. Lett.* **1951**, *81*, 385.
(93) Vosko, S. J.; Wilk, W.; Nusair, M. *Can. J. Phys.* **1980**, *58*, 1200.
(94) Becke, A. D. *J. Chem. Phys.* **1993**, *98*, 5648.
(95) Lee, C. T.; Yang, W. T.; Parr, R. G. *Phys. Rev. B* **1988**, *37*, 785.
(96) Cornehl, H. H.; Wesendrup, R.; Diefenbach, M.; Schwarz, H. *Chem.—Eur. J.* **2997**, *3*, 1083.
(97) Groenewold, G. S.; Cossel, K. C.; Gresham, G. L.; Gianotto, A. K.; Appelhans, A. D.; Olson, J. E.; Van Stipdonk, M. J.; Chien, W. *J. Am. Chem. Soc.* **2006**, *107*, 3075.
(98) Parsons, Z.; Leavitt, C.; Duong, T.; Groenewold, G. S.; Gresham, G. L.; Van Stipdonk, M. J. *J. Phys. Chem. A* **2006**, *110*, 11627.
(99) Aubriet, F.; Muller, J.-F.; Poleunis, C.; Bertrand, P.; Di Croce, P. G.; Grange, P. *J. Am. Soc. Mass Spectrom.* **2006**, *17*, 406.
(100) Chaoui, N.; Millon, E.; Muller, J. F. *Chem. Mater.* **1998**, *10*, 3888.
(101) Cossarutto, L.; Chaoui, N.; Millon, E.; Muller, J. F.; Lambert, J.; Alnot, M. *Appl. Surf. Sci.* **1998**, *126*, 352.
(102) Amoruso, S.; Bruzzese, R.; Spinelli, N.; Velotta, R. *J. Phys. B: At., Mol. Opt. Phys.* **1999**, *32*, R131.
(103) Bryantsev, S.; de Jong, W. A.; Cossel, K. C.; Diallo, M. S.; Goddard, W. A., III.; Groenewold, G. S.; Chien, W.; Van Stipdonk, M. J. *J. Phys. Chem. A* **2008**, *112*, 5777.
(104) Leavitt, C. M.; Bryantsev, V. S.; de Jong, W. A.; Diallo, M. S.; Goddard, W. A., III.; Groenewold, G. S.; Van Stipdonk, M. J. *J. Phys. Chem. A* **2009**, 113.
(105) Albaret, T.; Finocchi, F.; Noguera, C. *Appl. Surf. Sci.* **1999**, *144−145*, 672.
(106) Chesnavich, W. J.; Su, T.; Bowers, M. T. *J. Chem. Phys.* **1980**, *72*, 2641.
(107) Su, T.; Bowers, M. T. *J. Am. Chem. Soc.* **1973**, *95*, 7611.
(108) Su, T.; Bowers, M. T. *J. Am. Chem. Soc.* **1973**, *95*, 7609.
(109) Su, T.; Bowers, M. T. *Int. J. Mass Spectrom. Ion Phys.* **1973**, *12*, 347.
(110) Su, T.; Bowers, M. T. *Int. J. Mass Spectrom. Ion Phys.* **1975**, *17*, 211.
(111) Su, T.; Chesnavich, W. J. *J. Chem. Phys.* **1982**, *76*, 5183.
(112) Su, T.; Su, E. C. F.; Bowers, M. T. *J. Chem. Phys.* **1978**, *69*, 2243.

JP9015432